CHAPTER IV
RESULTS AND DISCUSSION

4.1 Catalyst Characterization

4.1.1 Elemental Analysis by XRF

Table 4.1 shows the chemical compositions obtained from XRF analyses, expressed as weight percentages, of the investigated catalysts. As mentioned in methodology, the theoretical Ce/Zr mole ratio of 3:1 and vary Ni loading (5, 10, 15 and 25 wt%). The results showed that both preparation methods yield similar Ni doped CZO catalysts with Ce/Zr molar ratio close to the theoretical ones.

Table 4.1 Elemental analysis results for the catalysts synthesized

Catalyst	Composition (wt%)				Mole Ratio of Ce/Zr
	Ce	Zr	Ni	O	
CZO	66.42	13.91	n/a	19.67	3.11
5Ni/CZOi	62.86	12.87	5.12	19.15	3.18
10Ni/CZOi	61.56	11.48	9.89	17.07	3.49
15Ni/CZOi	60.96	12.18	14.94	11.92	3.26
25Ni/CZOi	56.83	11.87	24.72	6.58	3.12
5Ni/CZOp	62.61	12.97	5.08	19.34	3.14
10Ni/CZOp	60.62	11.52	10.12	17.74	3.43
15Ni/CZOp	59.42	12.65	13.8	14.13	3.06
25Ni/CZOp	55.71	10.82	24.87	8.6	3.35

*CZO =Ce75Zr25Ox

The catalysts synthesized are designated as mNi/CZOx where m represents the weight percentage and x represents either i (impregnation) or p (polyol mediated) method.

4.1.2 BET Surface Areas and Degrees of Metal Dispersion

BET surface areas, pore volumes of the investigated catalysts are shown in Table 4.2. The surface area of CZO support was ca. 92 m^2/g with total pore volume of 0.081cm^3/g. After Ni loading from 5 to 25 wt%, the BET surface area of the impregnated catalysts (Ni/CZOi) is in the range of 54-78m^2/g with total pore volumes of 0.132-0.145 cm^3/g while the BET surface area of the polyol mediated catalysts (Ni/CZOp) is in the range of 70-88 m^2/g with total pore volumes of 0.146-0.157 m^2/g. Since the surface areas and the total pore volumes of both types of catalyst are, respectively, decreased and increased when compared with that of CZO, it is postulated that Ni would disperse into the pores and also agglomerate on the external surface forming the opened clusters. However, a less decrease in surface area and a greater increase in total pore volume can be observed for the Ni/CZOp. As an increase in Ni loading, the volume of micropores is increased resulting from the pore blocking by the loaded metal. The higher BET surface area in case of polyol mediated catalysts it is noteworthy that polyol method has better control on distribution of active metal over support. The better distribution of active metal over support avoids pore blockage of support and produces catalyst with surface area and large pore volume.

The degree of metal dispersion of Ni/CZOp is higher than that of Ni/CZOi, corresponding to smaller crystallite size of NiO at a given Ni loading, which will be discussed in XRD section. For both preparation methods, the metal dispersion degree is found to decrease with increasing Ni loading. This might be due to the formation of NiO bulk particles (Shishido *et al.*, 2002).

Table 4.2 Textural properties and metal characteristics of the prepared catalysts.

Catalyst	BET Surface Area (m^2/g)	Total Pore Volume (cm^3/g)	Mesopore Volume (cm^3/g)	Micropore Volume* (cm^3/g)	Degrees of Metal Dispersion (%)	NiO Crystallite Size** (nm)
CZO	91.79	0.081	0.072	0.009	-	-
5Ni/CZOi	78.07	0.143	0.131	0.012	8.33	10.1
10Ni/CZOi	67.07	0.132	0.112	0.020	5.32	20.1
15Ni/CZOi	63.63	0.145	0.110	0.035	4.46	20.7
25Ni/CZOi	54.33	0.129	0.091	0.038	2.34	24.7
5Ni/CZOp	88.19	0.153	0.143	0.010	9.07	6.7
10Ni/CZOp	80.97	0.146	0.125	0.021	7.54	7.1
15Ni/CZOp	78.14	0.157	0.112	0.045	6.82	9.0
25Ni/CZOp	70.06	0.149	0.099	0.050	3.87	11.7

*Using t-method, **Determined from XRD results

4.1.3 X-ray Diffraction (XRD)

XRD patterns for the prepared catalysts are shown in Figure 4.1. All catalysts exhibit major peaks at ca. 28.5°, 33.1°, 47.4°, and 56.4° (2θ) of a cubic fluorite CeO_2 structure. Some extra peaks of tetragonal phase due to non-incorporated ZrO_2 are observed at ca. 30.0°, 50.3° and 59.4° (2θ). This is probably because small amounts of Zr species were not incorporated into the CeO_2 lattices (Pengpanich *et al.*, 2002). Crystalline phases of NiO are present at ca. 37.3°, 43.4°, 63.0°, and 77.0° (2θ).

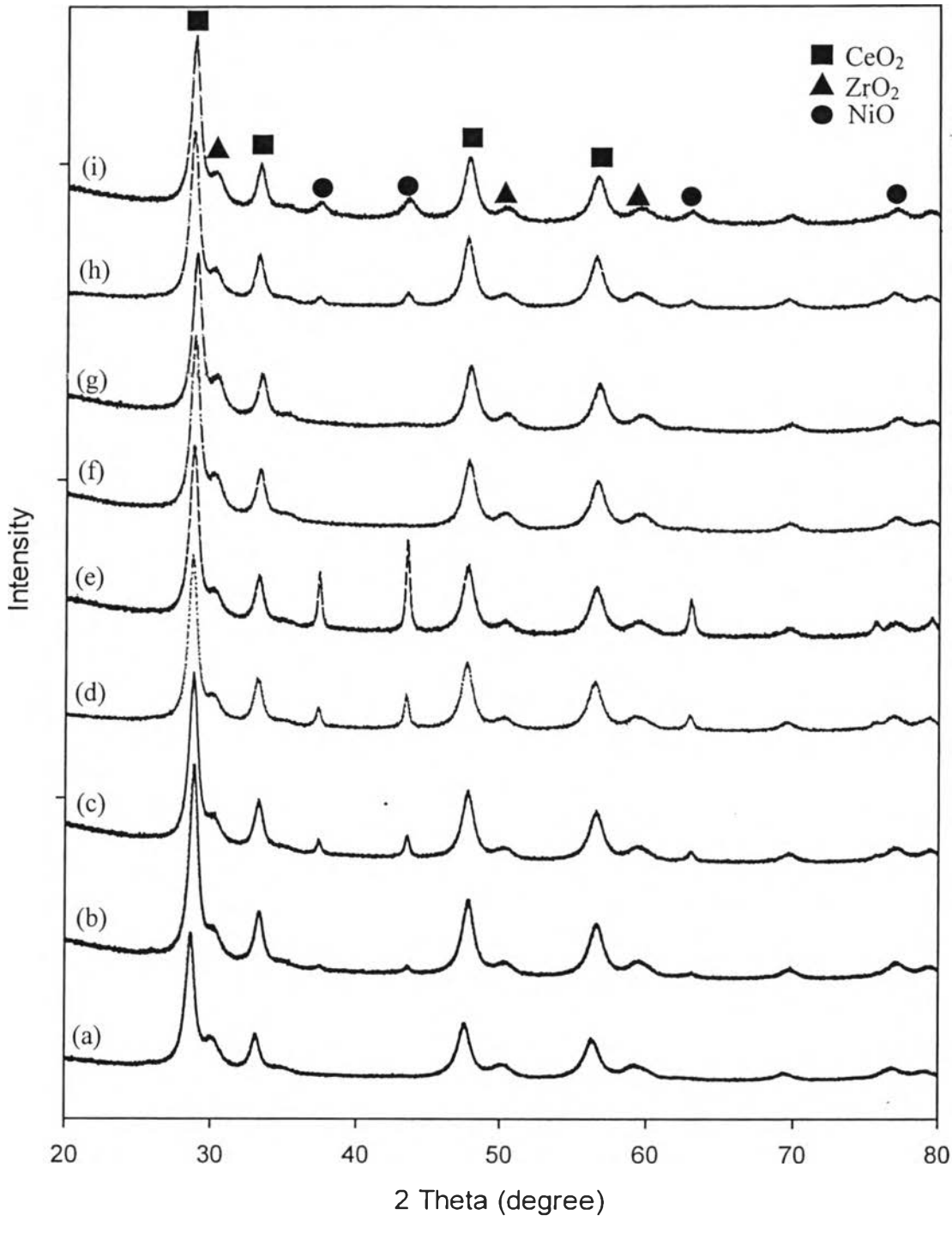

Figure 4.1 XRD patterns of the catalysts: a) CZO, (b) 5Ni/CZOi, (c) 10Ni/CZOi, (d) 15Ni/CZOi, (e) 25Ni/CZOi, (f) 5Ni/CZOp, (g) 10Ni/CZOp, (h) 15Ni/CZOp and (i) 25Ni/CZOp.

For the impregnated catalysts, the peak intensity of NiO is obviously stronger with increasing Ni loading suggesting that, at a low Ni content, NiO was present in form of nanoparticles while, at a high Ni content, bulk NiO agglomerated particles were present (Zhu and Flytzani-Stephanopoulos, 2001). For the polyol mediated catalysts, the peaks become broader than those of the impregnated catalysts at the same Ni loading. The absence of NiO peak in cases of 5 and 10Ni/CZOp might be due to the low metal loading or smaller metal particle size less than the detection limit of XRD. The sizes of NiO crystallites were calculated by Scherrer equation. However, the NiO crystallite size of Ni/CZOp is in the range of ca. 7-12 nm whereas that of Ni/CZOi is in the range of ca. 10-25 nm as shown in Table 4.2. The presence of smaller crystallite, in case of polyol mediated catalysts is actually credited to high and controlled dispersion of Ni species over support.

4.1.4 Temperature-programmed Reduction of Hydrogen (H_2-TPR)

H_2-TPR experiments were carried out to investigate the reducibility as well as the interaction between Ni species and support for both Ni based impregnated and polyol mediated catalysts. H_2-TPR profiles for the catalysts are presented in Figure 4.2. The TPR profile for CZO indicates a typical reduction peak of CeO_2 at ca. 450 °C. The H_2-TPR profiles for all catalysts exhibit two major reduction peaks. The first peak at lower temperature is attributed to the reduction of NiO particles interacting weakly with support and the second peak at higher temperature is ascribed to the reduction of NiO particles interacting strongly with support (Roh *et al.*, 2002). Furthermore, the shoulder peak is attributed to the partial reduction of Ce^{4+} to Ce^{3+} (Larimi *et al.*, 2012).

An increase in Ni loading insignificantly influences the reduction temperature of NiO over CZO mixed oxide support for individual methods. The reduction peaks for the catalyst become increasing intensity with increasing Ni loading indicating more nickel species located on the outer surface of the support and are easier accessible, and therefore the reducibility of nickel species is promoted (Zhikun *et al.*, 2012). For 25Ni/CZOi and 25Ni/CZOp catalysts the first peak at lower temperature shifted to lower reduction temperature than the other mNi/CZOi and mNi/CZOp catalysts indicating some large NiO particles interacting quite weak

with support. The second peak at higher temperature shifted to higher reduction temperature for 25Ni/CZOi catalyst than for the other mNi/CZOi catalysts indicating the aggregation of nickel species forming large particles in size, which would induce slow hydrogen diffusion in nickel oxide phase, leading to a high reduction temperature. For 25Ni/CZOp catalyst, the peaks are insignificantly different from the other mNi/CZOp catalysts indicating highly dispersed metal over support resulting in suppressing nickel aggregation.

However, the Ni/CZOp catalysts have both peaks shifted to higher reduction temperatures than do the Ni/CZOi catalysts. This implies that the Ni/CZOp catalysts possessed stronger interaction between NiO and CZO support than the Ni/CZOi catalysts due to their higher metal dispersion.

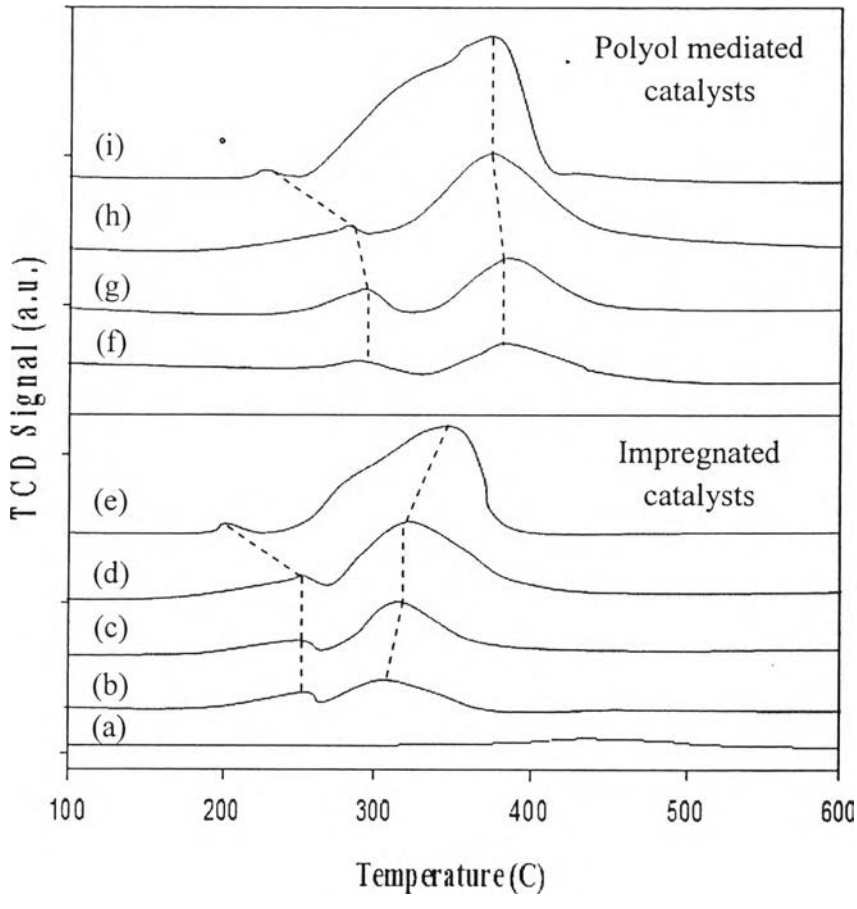

Figure 4.2 H_2-TPR profiles for supports with a heating rate of 10 °C/min, a reducing gas containing 5 % H_2 in Ar with a flow rate of 50 ml/min. : (a) CZO, (b) 5Ni/CZOi, (c) 10Ni/CZOi, (d) 15Ni/CZOi,(e) 25Ni/CZOi, (f) 5Ni/CZOp, (g) 10Ni/CZOp, (h) 15Ni/CZOp and (i) 25Ni/CZOp.

4.1.5 Scanning Electron Microscopy (SEM)

Figure 4.3 shows SEM images of all the catalysts investigated. For the Ceria-Zirconia mixed oxide support presents a morphology which is the aggregation of the primary long thin needle shaped particles (Thammachart *et al.*, 2001). The morphology of the Ni-doped catalysts was similar to CZO mixed oxide support covering with particles of the NiO particle attached onto the surface of supports.

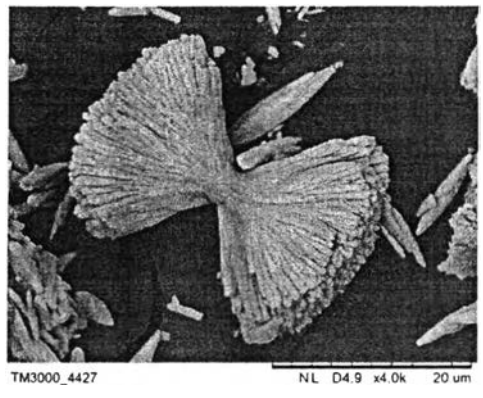

(a)

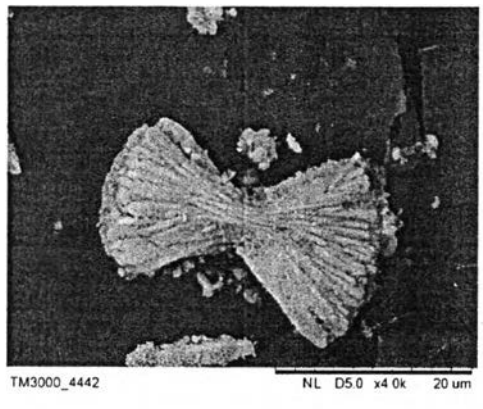

(b)

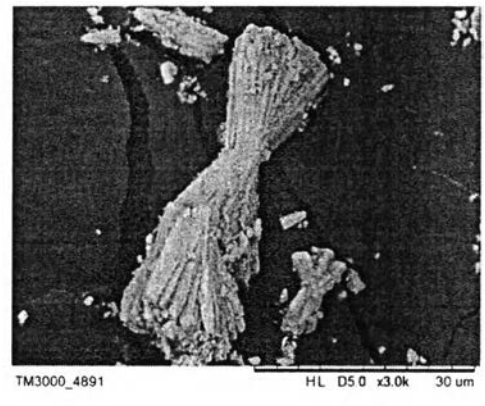

(c)

Figure 4.3 SEM images of a) CZO, b) Ni/CZOi, and c) Ni/CZOp.

4.2 Catalytic Activities for Catalytic Partial Oxidation of Methane

4.2.1 Catalytic Activities for CPOM

The catalytic partial oxidation of methane (CPOM) was carried out over all catalysts under the following conditions: CH_4/O_2 molar ratio of 2:1 balance with He, total flow rate 100 ml/min and at atmospheric pressure. xNi/CZO catalysts (where x = 5, 10, 15 and 25 wt%) were prepared by incipient wetness impregnation and polyol mediated method to investigate the effect of NiO crystallite size and metal dispersion in the CPOM reaction.

As shown in Figures 4.4 and 4.5, CH_4 conversion and CO_2 yield slowly increase with increasing temperature between 400 and 550 °C which proved the exothermic property of methane combustion reaction ($CH_4 + 2O_2 \rightarrow CO_2 + 2H_2O$, ΔH= -803 kJ/mol) with CO_2 and H_2O as complete oxidation products. It is distinguishable at 400 °C that methane conversion for all the polyol catalysts rises although there are no appearances of H_2 and CO (Figures 4.6 and 4.7, respectively). This implies that the polyol catalysts are more active for catalytic combustion at lower temperatures (< 550 °C) than the impregnated ones. This is due to its smaller NiO crystallite size explained by XRD results and higher metal dispersion which were discussed in previous section. Above 600 °C, CH_4 conversion was rapidly increased and rather constant above 750 °C. The CO_2 yield was decreased due to the occurrence of the reforming of CO_2 ($CH_4 + CO_2 \rightarrow 2CO+2H_2$, ΔH=+226 kJ/mol), H_2O reaction with remaining methane ($CH_4 + H_2O \rightarrow 2CO + 3H_2$, ΔH=+261 kJ/mol) and the competition between reforming and Reverse Water Gas Shift (RWGS) reaction ($H_2+CO_2 \rightarrow H_2O+CO$, ΔH=-39.5 kJ/mol) which led to increase the CH_4 conversion and decrease the CO_2 yield. This is also resulted CO yield higher than H_2 yield as shown in Figures 4.6-4.7.

The results showed that all the catalysts prepared by polyol mediated technique (polyol mediated catalysts) exhibit higher methane conversion than those prepared by impregnation method (impregnated catalysts) at a given Ni loading and reaction temperature The CH_4 conversion, H_2 and CO yields were increased with temperature. The decreasing of the CH_4 conversion, H_2 and CO yields in case of 15Ni/CZOi at temperature above 750 °C due to the sintering of Ni metal and the

deactivation from coke formation. This is agreement with the weaker metal support interaction in TRP result. Both H_2 and CO yields are significantly attained for the polyol catalysts compared to the impregnated catalysts.

As shown in Figure 4.8 with increasing Ni loading from 5 to 15 wt%, the CH_4 conversion over all catalysts was increased because surface area of active site was increased. For the 25Ni/CZOp, CH_4 conversion was slightly decreased while CH_4 conversion was drastically decreased in case of 25Ni/CZOi. This might be increasing amount of Ni loading, Ni could generally be poorly dispersed and Ni crystallite size became much larger so led to decrease surface area of active site surface.

The H_2/CO ratio of the investigated catalysts at various temperatures was shown in Figure 4.9. The H_2/CO ratio of the Ni-doped catalysts was insignificant difference indicating the same pathway reaction. The H_2/CO was in range of 1.4-1.7 which is below the theoretical value of 2. This can be explained that there was the reverse water gas shift reaction ($CO_2+H_2 \rightarrow CO+H_2O$) occurring during the reaction. Moreover, it might be due to the CPOM did not directly occur ($CH_4+1/2O_2 \rightarrow CO + 2H_2$, H_2/CO ratio=2) but the reaction occur through the combustion reaction following by reforming which H_2/CO is not 2.

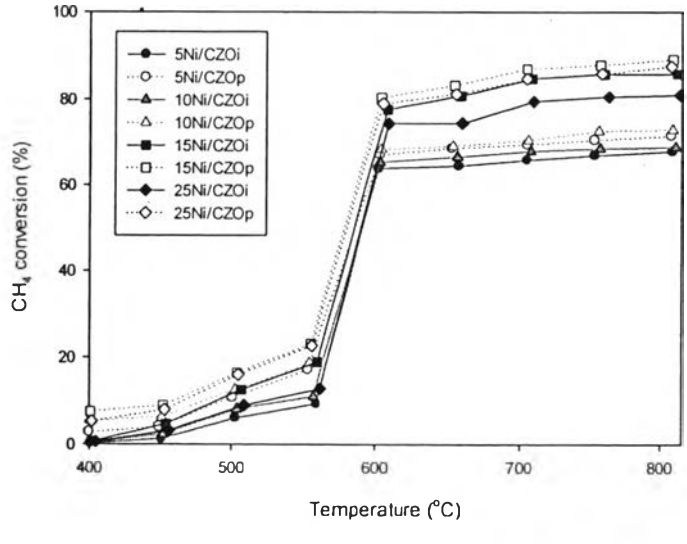

Figure 4.4 Methane conversion at various temperature over the investigated catalyst using CH_4/O_2 ratio = 2:1 and GHSV = 53000 h^{-1}.

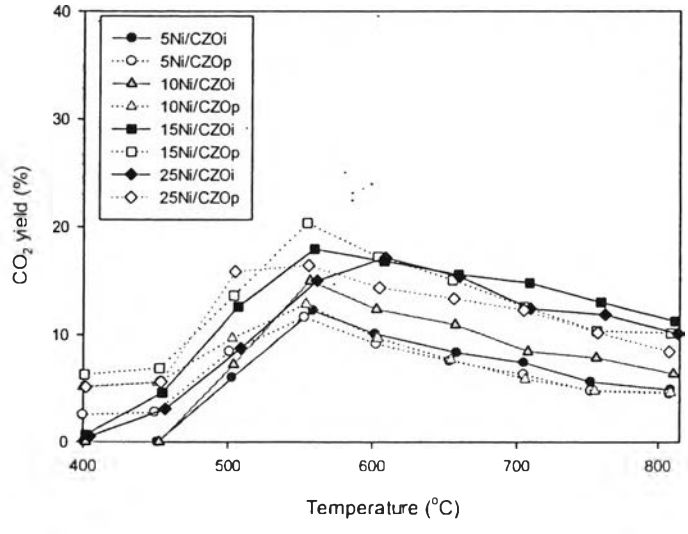

Figure 4.5 CO_2 yield at various temperature over the investigated catalyst using CH_4/O_2 ratio = 2:1 and GHSV = 53000 h^{-1}.

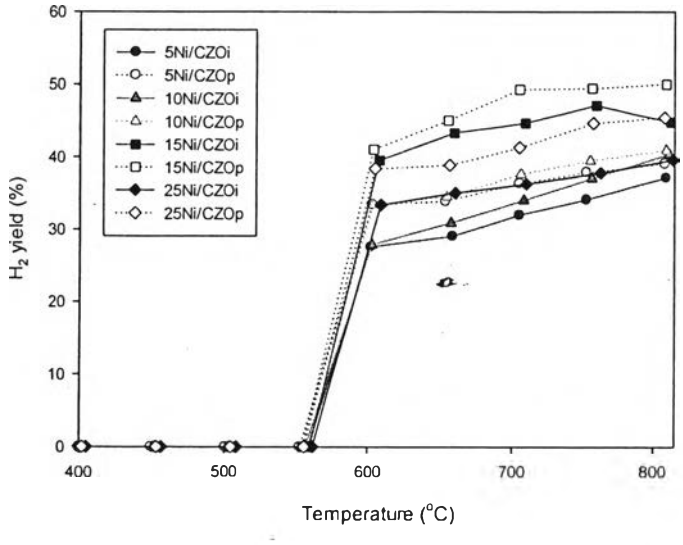

Figure 4.6 H_2 yield at various temperature over the investigated catalyst using CH_4/O_2 ratio = 2:1 and GHSV = 53000 h^{-1}.

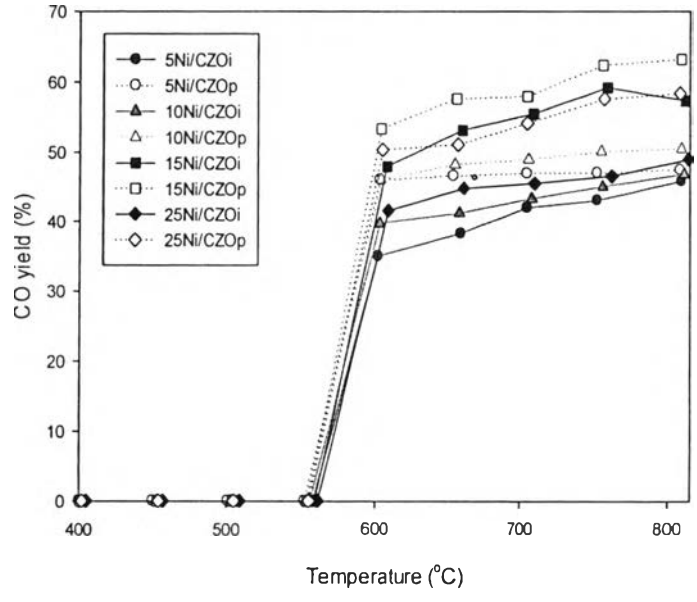

Figure 4.7 CO yield at various temperature over the investigated catalyst using CH_4/O_2 ratio = 2:1 and GHSV = 53000 h^{-1}.

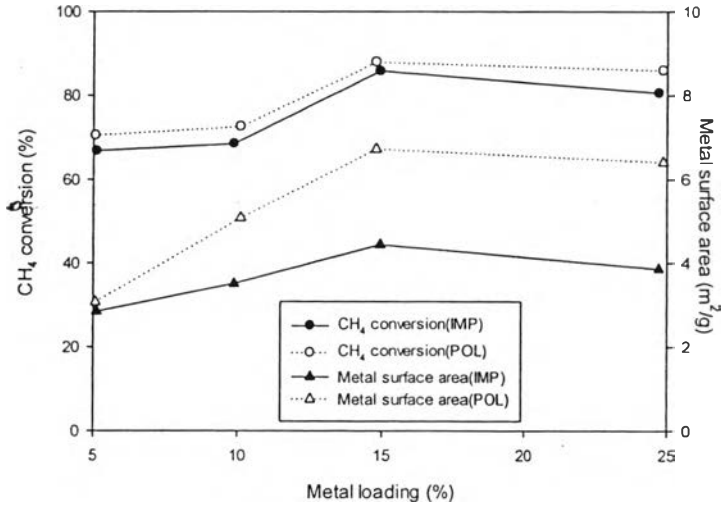

Figure 4.8 Methane conversion and metal surface area as a function of Ni loading at 750 °C using CH_4/O_2 ratio = 2:1 and GHSV = 53000 h^{-1}.

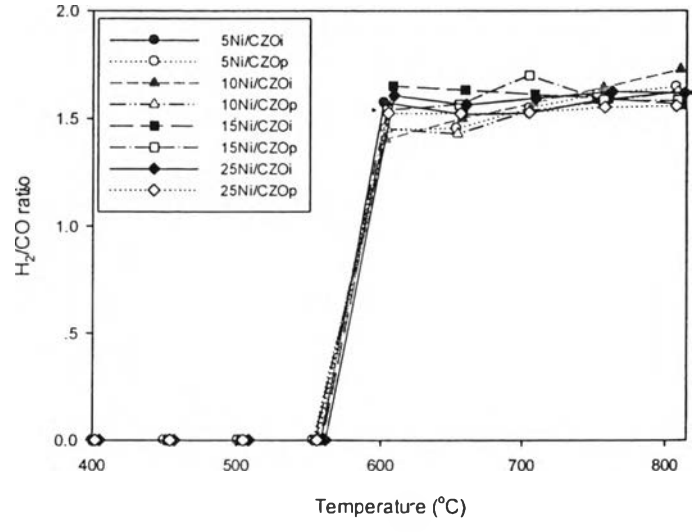

Figure 4.9 H_2/CO ratio at various temperature over the investigated catalyst using CH_4/O_2 ratio = 2:1 and GHSV = 53000 h^{-1}

4.2.2 Effect of CH_4/O_2 Ratio

From previously discussed, polyol mediated catalysts are active than impregnated catalysts. In order to make it obvious, the 15Ni/CZO catalysts were tested at severe condition by increasing CH_4/O_2 ratio to 4:1. As given in Figure 4.10-4.12, an increase in methane content in feed stream (CH_4/O_2=4.0), the CH_4 conversion, H_2 and CO yield were slightly decrease for both catalysts. Due to an increasing CH_4/O_2 feed ratio, adsorbed methane on the catalyst surface might be increased, further inhibiting O_2 adsorption resulting combustion yields (CO_2 and H_2O) were decreased. The less CO_2 and H_2O were produced, the less reactant to react with the remaining methane. This was negative effect on the syngas yield and decreased methane conversion. Moreover, increasing CH_4/O_2 feed ratio, the CH_4 dissociative reaction becomes a dominant reaction (Pengpanich *et al.*, 2006) which led to coke precursor. However, the polyol catalyst showed still higher CH_4 conversion, H_2 and CO yields than impregnated catalysts. This indicated that the polyol mediated catalysts are more active than impregnated catalysts due to the better Ni dispersion and smaller NiO crystallite size.

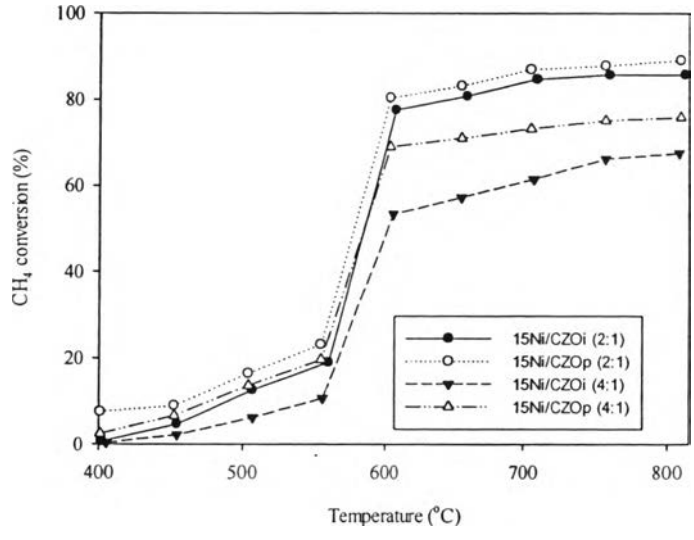

Figure 4.10 CH_4 conversion at various temperature over the investigated catalyst using CH_4/O_2 ratio = 2:1 and 4:1 and GHSV = 53000 h^{-1}.

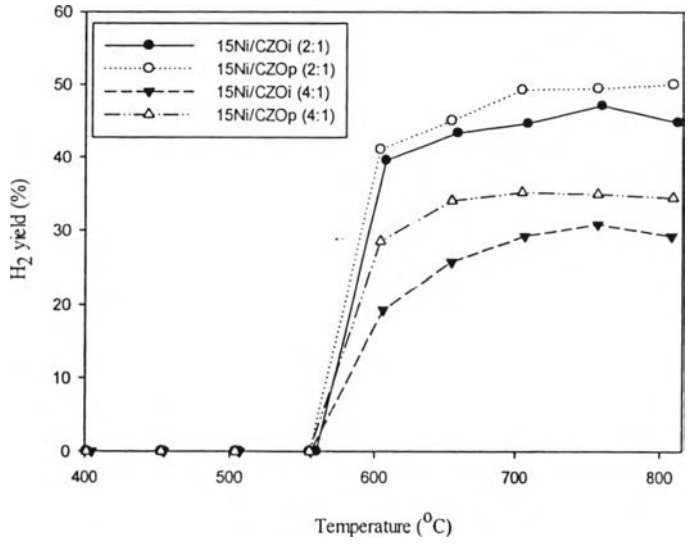

Figure 4.11 H_2 yield at various temperature over the investigated catalyst using CH_4/O_2 ratio = 2:1 and 4:1 and GHSV = 53000 h^{-1}.

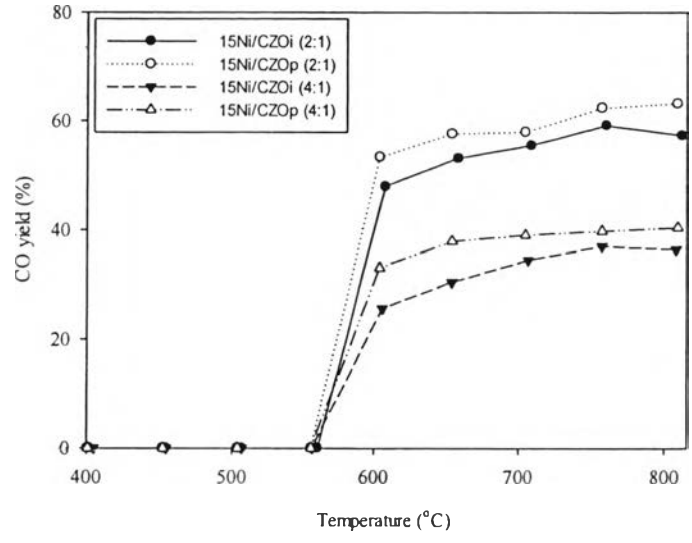

Figure 4.12 CO yield at various temperature over the investigated catalyst using CH_4/O_2 ratio = 2:1 and 4:1 and GHSV = 53000 h^{-1}.

4.2.3 Coke Formation on Catalyst and Catalyst Stability

In order to compare the long-term stability of polyol mediated catalysts and impregnated catalysts, the catalysts with 15 wt%Ni loading (15Ni/CZOi and 15Ni/CZOp) were tested for their stability at 750 °C, GHSV of 53000 h^{-1} with various of CH_4/O_2 ratio at 2.0 and 4.0, and atmospheric pressure.

As seen in Figures 4.13-4.16, the 15Ni/CZOp catalysts exhibits higher CH_4 conversion than the 15Ni/CZOi catalysts at both feed ratio. Noticeably, the 15Ni/CZOp catalyst seems to be invariably active even under a more severe reaction condition (CH_4/O_2 ratio of 4:1) for 6 h. H_2 selectivity of both catalysts remain unchanged over time investigated while their CO and CO_2 selectivity were slightly decreased and increased, respectively with increasing time on stream due to the Boudouard reaction ($2CO \rightarrow C+CO_2$) and methane decomposition reaction ($CH_4 \rightarrow C+H_2$) might occur during the course of reaction. The H_2/CO ratio of all investigated catalysts was insignificant change with time on stream.

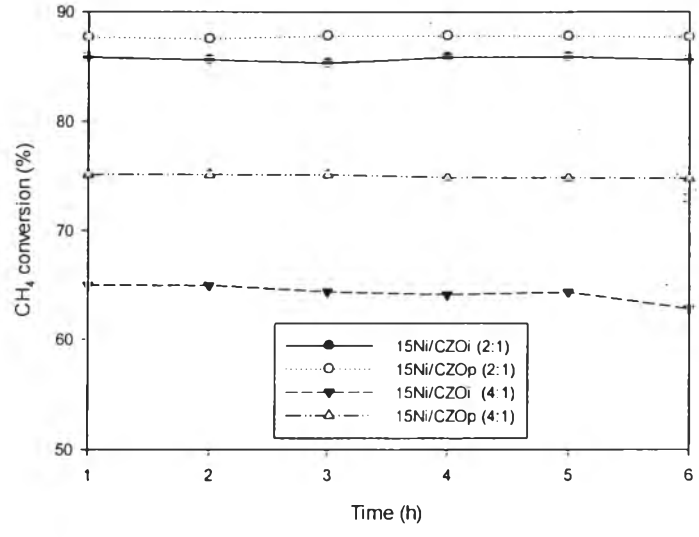

Figure 4.13 CH_4 conversion as a function of time over the catalysts investigated at 750 °C (CH_4/O_2 ratio of 2.0 and 4.0, GHSV=53000 h^{-1}).

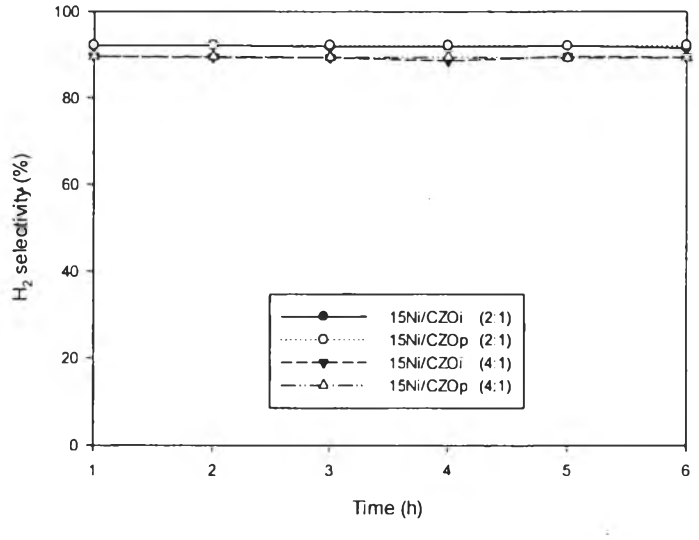

Figure 4.14 H_2 selectivity as a function of time over the catalysts investigated at 750 °C (CH_4/O_2 ratio of 2.0 and 4.0, GHSV=53000 h^{-1}).

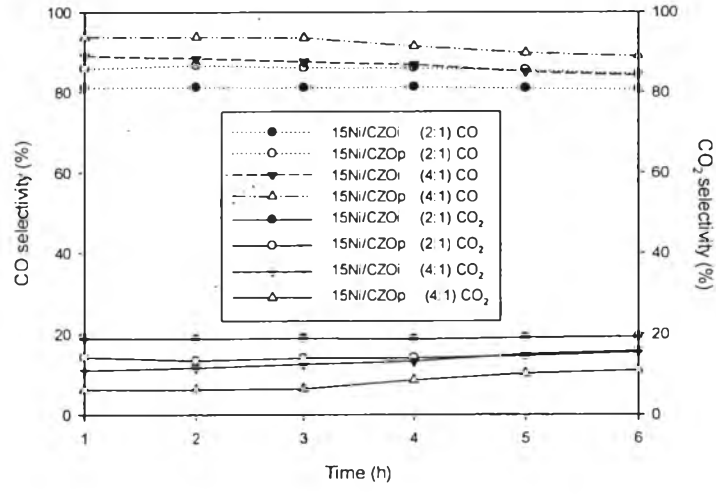

Figure 4.15 CO and CO_2 selectivities as a function of time over the catalysts investigated at 750 °C (CH_4/O_2 ratio of 2.0 and 4.0, GHSV=53000 h^{-1}).

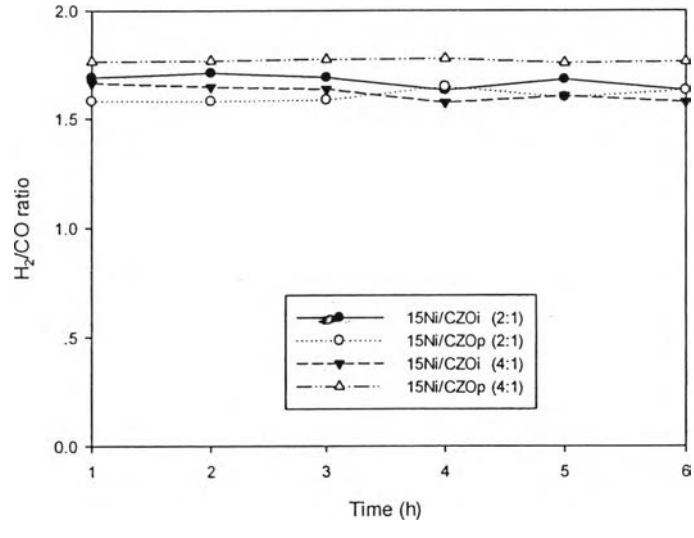

Figure 4.16 H_2/CO ratio as a function of time over the catalysts investigated at 750 °C (CH_4/O_2 ratio of 2.0 and 4.0, GHSV=53000 h^{-1}).

The coke formation has long been recognized as the main reason for catalyst deactivation in methane partial oxidation. Li *et al.*, (2004) reported that the rate of coke formation on catalyst surface is dependent on the relative rates of the carbon formation and its oxidative removal. Hence, if the rate of the carbon gasification by CO_2 is less than the rate of carbon formation, the large volume of carbon deposit will accumulate over gas–metal interface, which can afterward polymerize. These polymerized carbon atoms can contribute to catalysts deactivation via two ways: (i) encapsulating the active metal particles or diffusing through the active metal after dissolving, and (ii) detaching active metal particles from the support. Moreover, there are four possible reactions which favor coke formation is methane decomposition/cracking reaction ($CH_4 \leftrightarrow C + 2H_2$), CO disproportionation, i.e., Boudouard reaction ($2CO \leftrightarrow C + CO_2$), CO/H_2 reduction reaction ($CO + H_2 \leftrightarrow C + H_2O$) and CO_2 hydrogenation reaction ($CO_2 + 2H_2 \leftrightarrow C + 2H_2O$) (Haag *et al.*, 2007). In case of Ni based catalysts, the particle size of Ni is considered a dominant factor that determines the nature of coke formation. Additionally, coke formation occurs more easily on bigger particles than smaller ones (V. García *et al.*, 2009).

The results are in agreement with the amount of coke formation which obtained by TPO technique as shown in Figure 4.17 and Table 4.4. The TPO profile of catalysts shows two peaks at 370 and 520 °C indicating the amorphous and filamentous at lower and higher temperature, respectively. The results are similar to the observed by O¨zdemir *et. al.*, (2010) that when the TPO curves were investigated, at least two peaks were observed and the peak maxima were seen at higher temperatures than 400 °C. These peaks indicate that two or three different types of carbon were deposited on the catalysts. The amount of coke formation on the 15Ni/CZOi spent catalysts were 14.94 and 23.12 wt% for feed ratio of 2 and 4, respectively whereas 15Ni/CZOp spent catalysts were 10.78 and 18.21 wt% for feed ratio of 2 and 4, respectively. The coke formation increased with increased CH_4/O_2 feed ratio due to large amount of coke precursor which occurred from CH_4 dissociation. However, the polyol mediated catalysts has less coke formation than impregnated catalysts. This indicated that the strong interaction between Ni articles and mixed oxide support could prevent the agglomeration of Ni particles, which help

suppressing the coke formation on the catalysts. Due to the carbon formation is easy to deposit on a larger ensemble of active Ni sites (Trimm *et al.*, 1990). Moreover, the highly dispersed nano Ni particles obtained from polyol method decrease the structure defects and hence reduce the tendency of carbon to accumulate or diffuse into Ni particles.

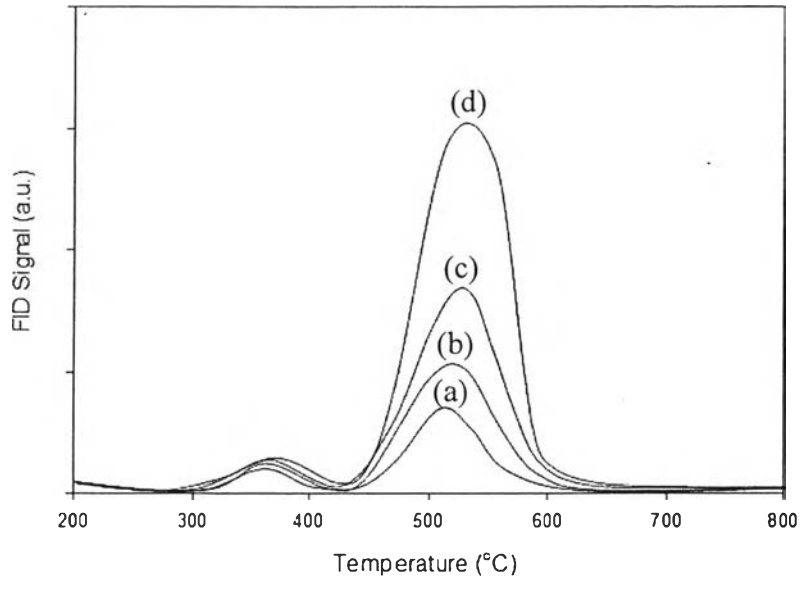

Figure 4.17 TPO profiles of catalysts after reaction at 750 °C (CH_4/O_2 ratio of 2.0 and 4.0, GHSV=53000 h^{-1}) an oxidizing gas containing 2% O2 in He with a flow rate of 40 ml/min: (a) 15Ni/CZOp (2:1), (b) 15Ni/CZOp (4:1), (c) 15Ni/CZOi (2:1), and (d) 15Ni/CZOi (4:1)

Table 4.3 Amounts of carbon deposited on the catalysts

Catalyst	CH_4/O_2 ratio	Amount of coke (wt.%)
15Ni/CZOi	2.0	14.94
	4.0	23.12
15Ni/CZOp	2.0	10.78
	4.0	18.21

As shown in Figure 4.18 the morphology of coke formation was investigated by TEM technique. For 15Ni/CZOp, the TEM observations showed the presence of both filamentous, within a diameter range of 7-40 nm and amorphous carbon which agree with TPO results. The filamentous carbon formed by the diffusion of carbon atoms through Ni particles which resulting in detaching Ni particles from the support being at the middle and at the top of the filament. Meanwhile 15Ni/CZOi, the TEM showed the presence of carbon coated Ni aggregates and filamentous within a diameter range of 13-60 nm. Dark spots in the TEM images correspond to the nickel clusters. It was observed that the diameter of filament in case of 15Ni/CZOp was smaller than those of 15Ni/CZOi. It was reported by Sakae *et al.* (2003) and Tang *et al.* (2001) that diameter of filament is controlled by diameter of metallic particles size. These results were in agreement with the results from XRD, which 15Ni/CZOp consists of smaller Ni particle size. Moreover, the carbon coated Ni aggregates in case of 15Ni/CZOi indicated the weak metal support interaction, which led to Ni sintering easily at high temperature, which corresponded with TPR results.

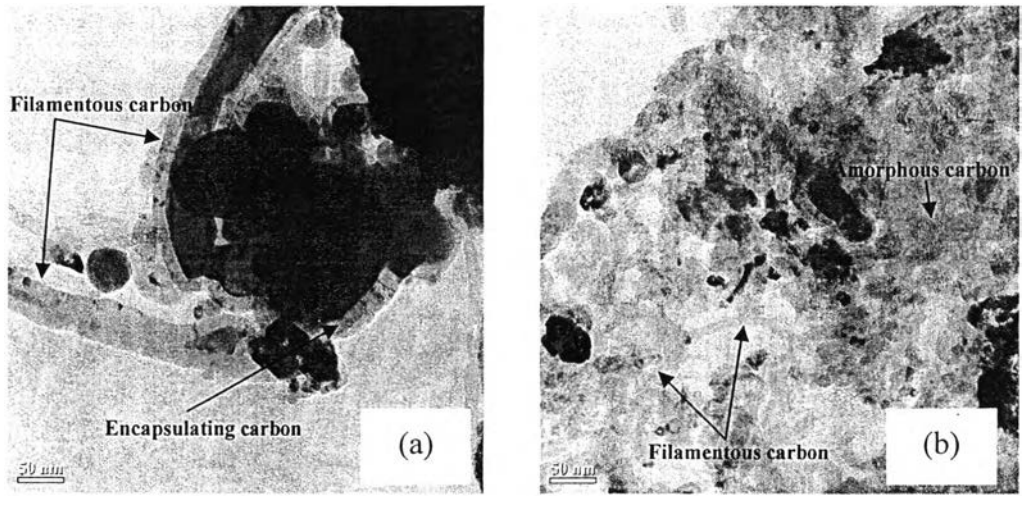

Figure 4.18 TEM images of spent catalysts after exposure to reaction at 750 °C (CH_4/O_2=2.0, GHSV=53000 h^{-1}): a) 15Ni/CZOi and b) 15Ni/CZOp